

Received November 17, 2018, accepted November 30, 2018, date of publication December 20, 2018, date of current version January 23, 2019.

Digital Object Identifier 10.1109/ACCESS.2018.2888868

Latency-Optimal mmWave Radio Access for V2X Supporting Next Generation Driving Use Cases

SHAO-YU LIEN¹, YEN-CHIH KUO², DER-JIUNN DENG³, (Member, IEEE),
HUA-LUNG TSAI⁴, ALEXEY VINEL⁵, (Senior Member, IEEE),
AND ABDERRAHIM BENSLIMANE⁶, (Senior Member, IEEE)

¹Department of Computer Science and Information Engineering, National Chung Cheng University, Chiayi 62102, Taiwan

²Department of Electronic Engineering, National Formosa University, Yulin 63201, Taiwan

³Department of Computer Science and Information Engineering, National Changhua University of Education, Changhua 50074, Taiwan

⁴Industrial Technology Research Institute, Hsinchu 31057, Taiwan

⁵School of Information Technology, Halmstad University, 301 18 Halmstad, Sweden

⁶Department of Computer Science, University of Avignon, 84029 Avignon, France

Corresponding author: Der-Jiunn Deng (derjiunn.deng@gmail.com)

This work was supported in part by the Ministry of Science and Technology (MOST) under Contract MOST 106-2221-E-194-065-MY2 and Contract MOST 107-2218-E-009-046, and in part by the Advanced Institute of Manufacturing with High-Tech Innovation (AIM-HI) from the Featured Area Research Center Program within the Framework of the Higher Education Sprout Project by the Ministry of Education (MOE) in Taiwan.

ABSTRACT With the facilitation of the fifth generation new radio, vehicle-to-everything applications have entered a brand new era to sustain the next generation driving use cases of advanced driving, vehicle platooning, extended sensors, and remote driving. To deploy these driving use cases, the service requirements, however, include low latency, high reliability, and high data rates, which thus render utilizing millimeter wave (mmWave) carriers (spectrum above 6 GHz) as a remedy to empower the next generation driving use cases. However, suffering from severe signal attenuation, the transmission range of mmWave carriers may be very limited, which is unfavorable in mobile network deployment to offer seamless services, and compel directional transmission/reception using beamforming mandatory. For this purpose, both a transmitter and a receiver should sweep their beams toward different directions over time, and a communication link can be established only if a transmitter and a receiver arrange their beam directions toward each other at the same time (known as beam alignment). Unfortunately, the latency of performing beam sweeping to achieve beam alignment turns out to be a dominating challenge to exploit mmWave, especially for the next generation driving use cases. In this paper, we consequently derive essential principles and designs for beam sweeping at the transmitter side and receiver side, which not only guarantee the occurrence of beam alignment but also optimize the latency to achieve beam alignment. Based on the availabilities of a common geographic reference and the knowledge of beam sweeping scheme at the transmitter side, we derive corresponding performance bounds in terms of latency to achieve beam alignment, and the device corresponding latency-optimal beam sweeping schemes. The provided engineering insights, therefore, pave inevitable foundations to practice the next generation driving use cases using mmWave carriers.

INDEX TERMS NR V2X, next generation driving use cases, mmWave, low latency, beam sweeping.

I. INTRODUCTION

Different from conventional vehicular communication technologies, such as IEEE 802.11p Dedicated Short Range Communications (DSRC) [1]–[4] and 3GPP Long-Term Evolution Advanced (LTE-A) Vehicle-to-Everything (V2X) [5]–[7], mainly targeting at scenarios of electronic toll collection (ETC), safety message exchanges, urgent event awareness, commercial transactions on vehicles, etc., 3GPP has envisioned the next generation driving use cases since

Jun. 2018 [8], [9]. In 3GPP's vision, 28 use cases and corresponding service requirements are revealed to empower advanced intelligent transportation systems (ITS) [8]. These advanced driving use cases are classed into four major categories, including advanced driving, vehicle platooning, extended sensors and remote driving [9].

Since 28 use cases are involved, the service requirements (this part will be surveyed in Section II) are diverse to include low latency, ultra-high reliability and high data rates for

periodic and aperiodic traffic transmissions. As supporting ultra-reliable and low latency communications (URLLC) is one of the crucial features of 3GPP “New Radio (NR)” [10], 3GPP has launched a new normative work for NR V2X in Release 16 since 2018. Although these four categories specifically schematize the scope of upcoming ITS, sustaining these four categories over Release 16 is an extremely challenging task due to the following two issues.

A. OBSTACLES IN SUPPORTING HIGH RELIABILITY, LOW LATENCY AND HIGH DATA RATE V2X TRANSMISSIONS

First, to potentially sustain both periodic and aperiodic traffic transmissions, a gNB may not know when messages to be transmitted from a vehicle arrive at a vehicle. As a result, a vehicle needs to request radio resources from a gNB when it has messages to be delivered. However, to provide low latency message delivery, a vehicle may not rely on the conventional four-message exchanging procedure to request radio resource from a gNB, which may lead to unacceptably large latency. To avoid the four-message exchanging procedure, a new semi-persistent resource reservation scheme is introduced in Release 15 NR, in which a gNB semi-persistently reserves radio resources for a vehicle (that is, available transmission opportunities occur periodically for a vehicle). In this case, the latency to deliver messages is directly proportional to the time duration between the time instant when messages arrive at a vehicle and the time instant of the upcoming transmission opportunity). As a result, if transmission opportunities occur frequently over time, then the latency can be significantly reduced. On the other hand, if a vehicle does not have any message to be transmitted, then the reserved radio resources are wasted. Consequently, there is a tradeoff between latency and the amount of utilized radio resources. Second, to jointly sustain high reliability and low latency, the hybrid automatic repeat request (HARQ) to retransmit a message when the previous message transmission is not successful may lead to ineligible latency [11]–[13]. This concern thus renders one-shot transmission repetition and conservative modulation and coding scheme (MCS) the effective approaches. Generally, when the number of repetition increases (and/or the modulation order and coding rate decrease), the reliability is also enhanced as well. Consequently, there is also a tradeoff between latency/reliability and the amount of utilized radio resources.

Above two issues reveal the same fact that, to support high reliability and low latency, more radio resources and thus more bandwidth are inevitably required. Together with the service requirements of high data rate transmissions, the remedy to support four categories of the next generation driving use cases turns out to exploit the millimeter-wave (mmWave) spectrum, where sufficiently wide bandwidth is available. To this end, spectrum ranges both below 6 GHz (known as frequency range 1, FR1) and above 6 GHz (known as frequency range 2, FR2) are supported by NR V2X in Release 16.

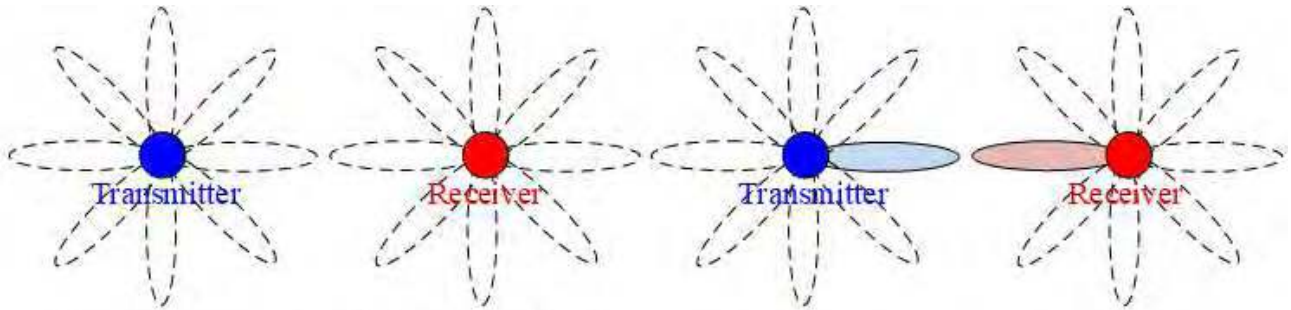
B. OBSTACLES IN EXPLOITING MMWAVE SPECTRUM FOR V2X TRANSMISSIONS

Although a wider bandwidth is available (up to 10-100 GHz) through exploiting mmWave spectrum, signal propagation may suffer from significant attenuation. As a result, the transmission range using mmWave spectrum may be very limited. In practice, a short transmission range may not be desired for V2X in providing seamless services. For this purpose, an operator should massively deploy a large number of (gNB-like) RSUs to eliminate potential coverage holes, which however leads to an unacceptable cost in deployment. In addition, to support high mobility up to 500 km/h, massive RSU deployment also invokes a large number of handovers, which renders service continuity a complicated issue. To address above engineering concerns, the transmission range of using mmWave spectrum should be substantially extended [14]–[17], and to this end, beamforming has been regarded as a mandatory function to apply mmWave to V2X use cases.

To extend the transmission range using beamforming, a transmitter may concentrate the transmission antenna gain on a certain beam (known as transmission beam) direction. In the meantime, a receiver may also concentrate the reception antenna gain on a certain beam (known as reception beam) direction. For this goal, a transmitter (or a receiver) may quantize its transmission (or reception) area into a certain number of beam directions, as illustrated in Fig. 1(a). A link between a transmitter and a receiver can be created only if the transmission beam direction and reception beam direction are arranged toward each other **at the same time**. This case is referred as *beam alignment*, as illustrated in Fig. 1(b). If both a transmitter and a receiver are aware of the geographic locations of each other, then beam alignment can be achieved through arranging the transmission beam direction toward the location of a receiver, and arranging the reception beam direction toward the location of a transmitter. Unfortunately, the locations of a transmitter and a receiver may not be a common knowledge when a vehicle just powers on or moves in the coverage of a RSU. At this moment, without any priori location knowledge of each other, both a RSU and a vehicle should sweep their transmission beam and reception beam over all possible beam directions, and this operation is known as *initial access*.

To perform initial access, there are two primary challenges having to conquer: (i) Both a transmitter and a receiver do not know which beam direction is able to achieve beam alignment due to the lack of the knowledge about the locations of each other. (ii) A transmitter and a receiver do not know the correct time to arrange the beam directions toward each other. To address these two challenges, three classes of beam sweeping schemes have received considerable attentions:

- **Signal to Interference and Noise Power Ratio (SINR) Maximization:** Both a transmitter and a receiver sweep their beams over all possible directions with an equal workload. Through proper designs of signal filtering and/or precoding architecture [18]–[22],

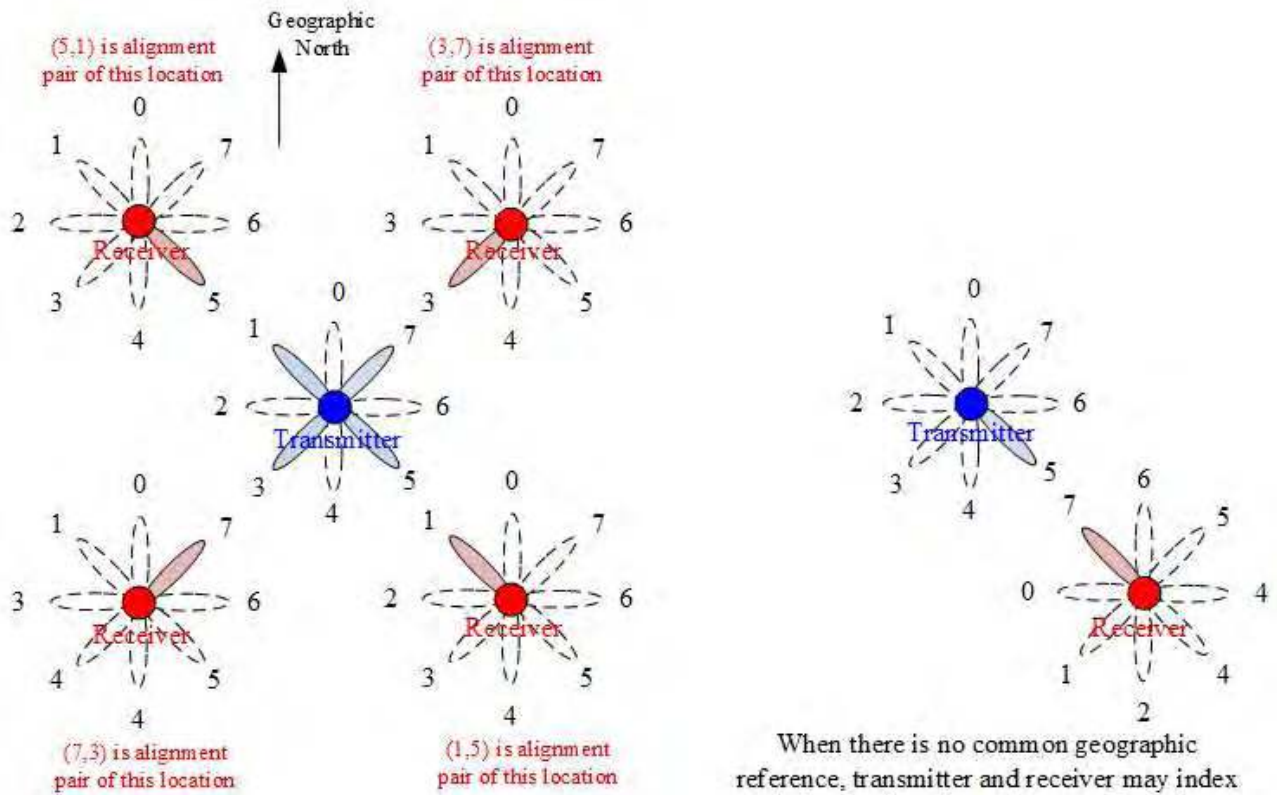


Both a transmitter and a receiver may quantize their transmission/reception areas into a certain number of beam directions

If transmission beam and reception beam sweep toward each other at the same time, beam alignment occurs.

(a)

(b)



Transmission beams and reception beam directions can be indexed according to common geographic location. At each location, there is a particular alignment beam pair.

When there is no common geographic reference, transmitter and receiver may index the beam direction on its own. Even the location of receiver does not change, if a receiver spins, (1,5) is no longer the alignment pair of this location

(c)

(d)

FIGURE 1. Beam sweeping at the transmitter side and receiver side to achieve beam alignment.

the locations of the transmitter and the receiver can be identified/estimated as the beam direction with the largest SINR. However, the concept of beam sweeping

sequence designs is not introduced in this class, and the beam sweepings at the transmitter side and receiver side only rely on exhaust search. As a result, it is

possible that the beam alignment could never be achieved. On the other hand, this class of designs also rely on a feedback channel for a receiver to inform the transmitter about the SINR of present beam direction arrangement. In addition, beam sweeping at the transmitter side and receiver side may need to be performed repeatedly to lead to a converged SINR results. Unfortunately, a feedback channel may not always exist especially for initial access. The repeated beam sweeping also extend the latency to achieve beam alignment.

- **Location Identification:** In this class of designs [23]–[26], particular tags, such as radio frequency identification (RFID) or global positioning system (GPS) are utilized by both a transmitter and a receiver to identify the locations of each other. However, information provided by RFID or GPS may not always be available for the radio layer to perform beam sweeping.
- **Open-Loop Sweeping:** Similar to the class of signal filtering, both a transmitter and a receiver sweep their beams over all possible directions with an equal workload. However, there is no feedback channel for a receiver to provide beam alignment information to a transmitter [26]–[31].

For practical deployment of V2X in which all vehicles may continuously change the locations, the “Open-Loop Sweeping” is the applicable design. For this class of designs, if the numbers of possible beam directions at the transmitter side and receive side are N_s and N_r , respectively, then the ideal latency to achieve beam alignment is $O(N_s N_r)$. However, existing beam sweeping designs do not guarantee beam alignment. If beam sweeping is not well designed, it is possible that beam alignment is never achieved. After the initial access, a moving vehicle may inherently change its location, and therefore beam sweeping should be continuously performed. Nevertheless, a vehicle may acquire information after initial access, such as a common geographic locations, to facilitate the optimization of the latency performance to achieve beam alignment for the *subsequent access* (SA).

C. CONTRIBUTIONS OF THIS PAPER

Despite the link vulnerability and beam alignment latency of applying the beamforming technology to moving vehicles, such directional transmission/reception has been regarded as the mandatory scheme to exploit FR2 spectrum, which is inevitable in practicing the four categories of the next generation driving use cases. Considering the ideal beam alignment latency $O(N_s N_r)$, effective designs of beam sweeping are thus urgently required to approach this ideal performance.

In this paper, we therefore derive the latency-optimal sweeping designs to achieve the ideal beam alignment latency $O(N_s N_r)$. Instead of providing a specific beam sweeping sequence, we derive the general principles to generate the latency-optimal beam sweeping sequence. The optimality of the derived principles is two-fold to a) guarantee that

beam alignment must occur within the sequence length of beam sweeping, and b) minimize the latency to achieve beam alignment. The performance evaluation results show that the beam sweeping sequences generated by the derived principle effectively guarantee the occurrence of beam alignment with the ideal latency of $O(N_s N_r)$.

II. SERVICE REQUIREMENTS OF THE NEXT GENERATION DRIVING USE CASES

The category of advanced driving supports automated driving of Society of Automotive Engineering (SAE) Level 3 to Level 6. For these medium to high degrees of automation, vehicles should share their status information (e.g., speed, heading) and action information (e.g., braking, acceleration, planned driving trajectory) with each other using direct device-to-device (D2D) communications [32], [33], to achieve cooperative collision avoidance (CoCA), emergency trajectory alignment, and cooperative lane change (CLC). The application layer to application layer (A2A) latency of message exchanges should be less than 3 to 25 ms. It implies that the Layer 1 latency should be less than 3 ms, with a reliability of 99.99%. For these information exchanges, messages are generated aperiodically, and the message size generally ranges from 300 bytes to 12000 bytes. In addition to information exchanges among vehicles, a vehicle may also exchange safety messages with a (gNB-like) road side unit (RSU) at intersections of roads. These safety messages include moving status and locations of pedestrians and vehicles, high-resolution (HD) digital map, and three-dimensional (3D) video. In generally, these safety messages are generated periodically with a generation rate of 10 messages per second. The message size ranges from 6000 bytes to 6500 bytes. The A2A latency to exchange these messages should be less than 100 ms, which implies that the Layer 1 latency should be less than 10 ms. In practice, at least 200 vehicles should be supported at each intersection. As a result, the message exchanges in this category can be periodic and aperiodic, with extremely low latency, high reliability, and high throughput.

The category of vehicle platooning can be regarded as a special case of advanced driving, in which multiple vehicles can form a platooning group with distance between vehicles less than 1 m. For this purpose, vehicles within a platooning group should share their status information and action information with other group members for cooperative maneuver. Therefore, the latency and reliability requirements of message exchanges in this category are similar to that of advanced driving. However, different from the message generation behavior in advanced driving that messages in some use cases are generated aperiodically, message generation in vehicle platooning is generally periodic with a generation rate ranges from 30 to 50 messages per second. As a result, the message exchanges in this category are periodic with extremely low latency, high reliability, and high throughput.

The category of extended sensors supports vehicles to perform cooperative perception, and in these use cases vehicles may share sensor or HD video data with other vehicles in

the same area. For this category, message generation is not required to be periodic, and therefore it can be generally aperiodic. The A2A latency requirement ranges from 3 ms to 50 ms, and therefore the Layer 1 latency should be less than 3 ms, with reliability ranging from 95% to 99.999%. Since the types of perception could be diverse, the message size may depend on the practical use cases. As a result, the message exchanges in this category are aperiodic with extremely low latency and high reliability.

The category of remote driving enables a vehicle to be controlled by either a person or cloud computing servers. When on-board cameras installed on a vehicle upload the live video to a remote person or cloud computing servers through RSUs, a remote person or cloud computing servers can send downlink vehicle control comments to a vehicle through RSUs. As a result, this category requires both uplink and downlink transmissions with an uplink data rate of 25 Mbps and a downlink data rate of 1 Mbps. The A2A latency should be less than 5 ms, which implies that the Layer 1 latency should be less than 2 ms, with a reliability of 99.999%. As a result, the message exchanges in this category are periodic in uplink and aperiodic in downlink with extremely low latency, high reliability, and high throughput in uplink.

III. SYSTEM CONSIDERATIONS

In this paper, we consider the latency-optimal beam alignment issue between a transmitter and a receiver. Suppose that a receiver has $N_r \geq 2$ possible beam directions indexed by $i = 0, \dots, N_r - 1$, and a transmitter has $N_s \geq 2$ possible beam directions indexed by $j = 0, \dots, N_s - 1$. Both a transmitter and a receiver are able to change their beam direction at each time t . Let $B_r(t)$ and $B_s(t)$ denote the selected beam directions at the receiver side and transmitter side at time t , respectively. Beam alignment can be achieved if a receiver sweeps its beam direction toward the location of a transmitter (denote this beam direction as i^*) and a transmitter sweeps its beam direction toward the location of a receiver (denote this beam direction as j^*), as illustrated in Fig. 1(a). In general, there is only one beam direction pair for a transmitter and a receiver to achieve beam alignment at each time t .

Definition 1: The minimum latency to achieve beam alignment is defined by

$$T = \inf\{t : B_r(t) = i^* \text{ and } B_s(t) = j^*\}. \quad (1)$$

Definition 2: A transmitter and a receiver sweep their beam directions with an equal workload if each beam direction is selected with an equal probability, i.e.,

$$\Pr\{B_r(t) = i\} = \frac{1}{N_r} \quad (2)$$

for all i , and

$$\Pr\{B_s(t) = j\} = \frac{1}{N_s} \quad (3)$$

for all j .

Due to the mobility nature of vehicles, the locations of both a transmitter and a receiver may change over time. Nevertheless, to achieve beam alignment, a transmitter and a

receiver only need to know the directions toward each other. Therefore, without loss of generality, we can assume that the location of a transmitter is fixed, and the location of a receiver, denoted by $Y_r(t)$, can change over time. In this case, the pair of transmission beam direction and reception beam direction to achieve beam alignment (i^*, j^*) may change over time as well. Let Z denote the number of possible locations where a receiver may move to (indexed by $z = 0, \dots, Z - 1$). To capture the mobility behavior of a receiver, let $\Pr\{Y_r(t) = z\} = y_z$ for all z denote the distribution of the location of a receiver. For any location where a receiver moves to, there is a corresponding pair of transmission beam direction and reception beam direction to achieve beam alignment, as illustrated in Fig. 1(c). Therefore, we can generally consider $Z = N_r$ and $\sum_{z=0}^{Z-1} y_z = 1$.

A. INITIAL ACCESS AND SA

At the initial access stage, there are two engineering concerns requiring to be taken into the design consideration.

- **A transmitter and a receiver are asynchronous in terms of beam sweeping sequence:** Since a transmitter may not know when a receiver may move in the transmitter's coverage, a transmitter may determine its own beam sweeping sequence without regarding the presence of a receiver. However, even though the beam sweeping sequence at the transmitter side can be defined in the specification to be common knowledge to a receiver, a receiver may not know the present beam direction of the transmitter, since a receiver may not know the beginning time when a transmitter launches beam sweeping.
- **A transmitter and a receiver may not always have a common geographic reference:** If a common geographic reference (such as geographic north) is available for both a transmitter and a receiver, then beam directions both at the transmitter side and receiver side can be indexed according to the common geographic reference. For example, both a transmitter and a receiver may index the beam direction toward the geographic North as 0, and increase the index counterclockwise, as illustrate in Fig. 1(c). In this case, at any location, there is a corresponding transmission beam direction j and a reception beam direction i to achieve beam direction, such as the beam pair ($i = 1, j = 5$) in Fig. 1(c). As a result, the total number of possible beam pairs to achieve beam alignment is limited to eight. However, if a common geographic reference is not available for a transmitter and a receiver, then a transmitter and a receiver may index their beam directions autonomously. Consequently, even though the location of a receiver does not change, if a receiver spins, then the original beam alignment pair ($i = 1, j = 5$) may no longer achieve beam alignment, as illustrated in Fig. 1(d). In this case, the total number of possible beam pairs to achieve beam alignment is 64.

To eliminate above two concerns, the following three remarks are essential for the latency-optimal beam sweeping designs.

Remark 1: For a latency-optimal beam sweeping design, the beam sweeping sequence at the transmitter side has to be periodic to facilitate a receiver to derive the beam direction of a transmitter. In other words, there exists a $L_s < \infty$ such that

$$B_s(t) = B_s(t + L_s), \quad (4)$$

where L_s is called the period of the beam sweeping sequence.

Remark 2: To guarantee the occurrence of beam alignment, the beam sweeping designs at the transmitter side and the receive side should guarantee the occurrence of all beam pairs. This implies that the beam sweeping sequence at the receiver side must also be periodic. In other words, there exists a $L_r < \infty$ such that

$$B_r(t) = B_r(t + L_r). \quad (5)$$

Remark 3: To guarantee the occurrence of beam alignment and to minimize the latency to achieve beam alignment, each combination of beam pairs should at least occur once within a finite duration. In addition, each combination of beam pairs should occur exactly once with a particular duration, and this duration is referred to as the **upper bound** of the beam alignment latency.

After the initial access stage, a receiver may continuously change its location. Therefore, beam sweeping should be performed continuously, which is known as SA as aforementioned. Fortunately, a receiver may obtain certain information at the initial access stage. On the other hand, if a receiver does not obtain any information from initial access, then the situation is identical to initial access. There can be two types of information: i) the availability of a common geographic reference, and ii) the availability of the beam sequence at the transmitter side. Based on these two information types, there can be four situations.

- **S1:** Only a common geographic reference is available, but not the beam sweeping sequence at the transmitter side.
- **S2:** Only the beam sweeping sequence at the transmitter side is available, but not a common geographic reference.
- **S3:** None of a common geographic reference and the beam sweeping sequence at the transmitter side is available.
- **S4:** Both of a common geographic reference and the beam sweeping sequence at the transmitter side are available.

For (S2) and (S3) in which a common geographic reference is not available, a receiver may not know which beam direction can achieve beam alignment even if a receiver has the knowledge about the beam sweeping sequence of a transmitter. As a result, these two situations degenerate to the initial access. Consequently, the beam sweeping sequence designs for initial access and SA can be harmonized, and we only need to emphasize on the designs in that case that a common geographic reference is available and case that a common geographic reference is unavailable.

IV. OPTIMUM BEAM SWEEPING SEQUENCES WHEN A COMMON GEOGRAPHIC REFERENCE IS UNAVAILABLE FOR S2 AND S3

When a common geographic reference is not available, **Remark 1** to **Remark 3** should be satisfied. For this purpose, a straightforward scheme is to adopt the **time shift sequences** at the transmitter side and receiver side [34]. For example, the beam direction 1 is selected at $t = 1$, the beam direction 2 is selected at $t = 2$, and the beam direction ($d \bmod N_s$ (resp. N_r)) is selected at $t = d$. In this manner, each combination of beam pairs occurs exactly once within $N_s N_r$ time slots. In fact, the time shift sequences are of multiple forms, and a general expression of the time shift sequences can be given by the following definition.

Definition 3: Let k_s and k_r denote the indices of the selected beam directions at the transmitter side and receiver side, respectively, at each time t , i.e.,

$$B_s(t) = k_s, \quad (6)$$

$$B_r(t) = k_r. \quad (7)$$

$B_s(t)$ and $B_r(t)$ are said to be time shift sequences if

$$k_s = (g_s t + b_s) \bmod p_s, \quad \text{for } t = 1, 2, \dots \quad (8)$$

$$k_r = (g_r t + b_r) \bmod p_r, \quad \text{for } t = 1, 2, \dots \quad (9)$$

where $g_s > 0$ and $g_r > 0$ are slopes of the sequences. $N_s \leq p_s \leq L_s$ and $N_r \leq p_r \leq L_r$ are lengths of the sequences. $0 \leq b_s \leq p_s - 1$ and $0 \leq b_r \leq p_r - 1$ are biases of the sequences.

An example provided in the following demonstrates how to apply different p_s , g_s and b_s to generate different forms of the beam sweeping sequences at the transmitter side.

Example 1: Consider a fixed $N_s = 5$. For $p_s = 5$, $g_s = 1$ and $b_s = 0$, the generated beam sweeping sequence is $B_s(t) = \{1, 2, 3, 4, 5, 1, 2, 3, \dots\}$. For $p_s = 5$, $g_s = 2$ and $b_s = 0$, the generated beam sweeping sequence is $B_s(t) = \{1, 3, 5, 2, 4, 1, 3, 5, \dots\}$. For $p_s = 5$, $g_s = 1$ and $b_s = 1$, the generated beam sweeping sequence is $B_s(t) = \{2, 3, 4, 5, 1, 2, 3, 4, \dots\}$. For $p_s = 6$, $g_s = 1$ and $b_s = 0$, the generated beam sweeping sequence is $B_s(t) = \{1, 2, 3, 4, 5, 1, 1, 2, 3, 4, 5, 2, 1, 2, 3, \dots\}$.

As a result, if the beam sweeping sequences are generated from the time shift sequences, then the generated beam sweeping sequences can be periodic. In the following lemma, the properties of the time shift sequences are characterized, which shows that if the beam sweeping sequences at the transmitter side and receiver side are generated using the time shift sequences, and if p_s and p_r are relatively prime numbers, then each combination of beam pairs occurs exactly once within $p_s p_r$.

Lemma 1: Let $\beta_s = \{0, 1, \dots, N_s - 1\}$ and $\beta_r = \{0, 1, \dots, N_r - 1\}$ denote the available sets of beam directions at the transmitter and receiver sides, respectively. The following properties hold if p_s and p_r are relatively prime numbers.

- i) For any integer d_s , $\beta_s \subset \{B_s(t + d_s), t = 1, 2, \dots, p_s\}$.

- ii) For any integer d_r , $\beta_r \subset \{B_r(t+d_r), t = 1, 2, \dots, p_r\}$.
- iii) Let $\beta_s \cup \beta_r = \{k_s, k_r : k_s = 0, 1, \dots, N_s - 1, k_r = 0, 1, \dots, N_r - 1\}$ be the set of all pairs of available transmission and reception beam directions. If p_s and p_r are relatively prime numbers, then $\{B_s(t+d_s), B_r(t+d_r)\} \subset \beta_s \cup \beta_r, t = 0, 1, \dots, p_s p_r - 1$, for any d_s and d_r .

Proof: The proof can be easily done through using the Chinese Remainder Theorem. ■

Although, in general, it can be $p_s \geq N_s$ and $p_r \geq N_r$, to minimize the latency to achieve beam alignment, p_s and p_r should be set to $p_s = N_s$ and $p_r = N_r$ in practice. From above lemma, if N_s and N_r are relatively prime numbers (and thus p_s and p_r are relatively prime numbers), then the occurrence of beam alignment can be guaranteed. As illustrated in Fig. 3, when N_s and N_r are not relatively prime numbers ($N_s = N_r = 4$), only a part of combinations of beam pairs occur. On the other hand, if N_s and N_r are relatively prime numbers ($N_s = 3$ and $N_r = 4$), then all combinations of beam pairs occur certainly. However, the practical values of N_s and N_r are designated by individual manufacturers, which are not guaranteed to be relatively prime numbers. In this case, the occurrence of beam alignment cannot be guaranteed either.

When N_s and N_r may potentially not be relatively prime numbers, p_s and p_r should be set to $p_s > N_s$ and $p_r > N_r$, respectively. To further ensure that p_s and p_r are relatively prime numbers, a common method is to introduce another M -bit cyclically unique codeword [35].

Definition 4: An M -bit codeword $(w(0), w(1), \dots, w(M-1))$ is cyclically unique if, for any cyclic shift x , the code word is not identical to $(w(x), w(x+1), \dots, w((M-1+x) \bmod M))$.

If a bit in the M -bit code is “0”, then a 0-sequence with period p_0 is generated from the time shift sequences. If a bit in the M -bit code is “1”, then a 1-sequence with period p_1 is generated from the time shift sequences. The slopes of both 0- and 1-sequences are set to 1, while the biases of both 0- and 1-sequences are set to 0. The final beam sweeping sequences at the transmitter side and receiver side are generated by interleaving M 0/1-sequences based on the values of an M -bit codeword.

Although M should be even, the size of M is not particularly restricted. We can assign the M -bit codewords to a transmitter and a receiver with an even length $M = 4$ as an example in practice.

Example 2: The 4-bit codewords at the transmitter side and the receiver side can be $\mathbf{w}_s = (w(0), w(1), w(2), w(3)) = (1, 1, 0, 0)$ and $\mathbf{w}_r = (w(0), w(1), w(2), w(3)) = (0, 1, 0, 1)$, respectively. The lengths of 0-sequence and 1-sequence at the receiver side are $p_{r,0} = N_r$ and $p_{r,1} = N_r + 1$, respectively. The lengths of 0-sequence and 1-sequence at the transmitter side are $p_{s,0} = N_s$ and $p_{s,1} = N_s + 1$, respectively.

Based on this example, the beam sweeping sequences at the transmitter side and receiver side can be generated according to the algorithms provided in the following. In these

Algorithm 1 Beam Sweeping Sequence Generation at Transmitter Side

Require: An available set of transmission beam directions β_s . The codeword length M is even and $M \geq 4$.

Ensure: A deterministic sweeping sequence $B_s(t) \in \beta_s$ for $t = 1, 2, \dots, H$, where $H > M$, is generated.

```

1: for  $t = 1$  to  $M$ 
2:   if  $t \neq 3$ ,  $B_s(t) = \text{fix}(\text{rand}(0, N_s - 1))$ 
3:   else  $t = 3$ ,  $B_s(3) = (B_s(1) + \lceil N_s/2 \rceil) \bmod N_s$ 
4: for  $t = M + 1$  to  $H$ 
5:   if  $t \bmod 2 = 1$ ,  $B_s(t) = B_s(t - M) + 1 \bmod p_{s,0}$ 
6:   else  $t \bmod 2 = 0$ ,  $B_s(t) = B_s(t - M) + 1 \bmod p_{s,1}$ 
7: for  $t = 1$  to  $H$ 
8:   if  $B_s(t) < N_s$ ,  $B_s(t) = B_s(t)$ 
9:   else  $B_s(t) = \alpha$ ,  $\alpha = (\alpha + 1) \bmod N_s$ 

```

Algorithm 2 Beam Sweeping Sequence Generation at Receiver Side

Require: An available set of reception beam directions β_r . The codeword length M is even and $M \geq 4$.

Ensure: A deterministic sweeping sequence $B_r(t) \in \beta_r$ for $t = 1, 2, \dots, H$, where $H > M$, is generated.

```

1: for  $t = 1$  to  $M$ 
2:    $B_r(t) = \text{fix}(\text{rand}(0, N_r - 1)) - 1$ 
3: for  $t = M + 1$  to  $H$ 
4:   if  $\lfloor (t \bmod 4) \bmod M/2 \rfloor = 1$ ,
5:      $B_r(t) = B_r(t - M) + 1 \bmod p_{r,0}$ 
6:   elseif  $\lfloor (t \bmod 4) \bmod M/2 \rfloor = 0$ ,
7:      $B_r(t) = B_r(t - M) + 1 \bmod p_{r,1}$ 
8: for  $t = 1$  to  $H$ 
9:   if  $B_r(t) < N_r$ ,  $B_r(t) = B_r(t)$ 
10:  else  $B_r(t) = \alpha$ ,  $\alpha = (\alpha + 1) \bmod N_r$ 

```

algorithms, $\text{rand}(0, N_s - 1)$ denotes taking a random number between 0 and $N_s - 1$, and $\text{fix}(\text{rand}(0, N_s - 1))$ denotes taking the integer part of $\text{rand}(0, N_s)$.

In **Algorithm 1** and **Algorithm 2**, we only design the beam sweeping sequence from $t = 1$ to H and the sequences repeat from $t = H + 1$ to $t = 2H$, and so on. In the following lemma, we analytically characterize H and show that each combination of beam pairs should occur exactly once within H . Please note that, in general the beam sweeping sequences at the sender side and receiver side are homogeneous for S2 and S3. Nevertheless, the sequence generation within $t = M + 1$ to H in **Algorithm 1** is different from that in **Algorithm 2**. This design leads to $N_s/2$ differences between the two 0-sequences at the transmitter side. We will elaborate later that this design further reduces latency in for S4.

Lemma 2: If a transmitter uses **Algorithm 1** and a receiver uses **Algorithm 2** to generate their beam sweeping sequences, then each combination of beam pairs occurs exactly once within

$$H = M \cdot \max(p_{r,0}, p_{s,1}) \max(p_{r,1}, p_{s,0}) \quad (10)$$

time slots.

Proof: This lemma can be proven by examining the following cases:

- **Case 1** ($p_{r,1} > p_{r,0} = p_{s,1} > p_{s,0}$): Since $p_{s,0}$ and $p_{r,1}$ are relatively prime numbers, the beam alignment time is $M \cdot p_{r,1} p_{s,0}$.
- **Case 2** ($p_{s,1} > p_{s,0} = p_{r,1} > p_{r,0}$): Since $p_{r,0}$ and $p_{s,1}$ are relatively prime numbers, the beam alignment time is $M \cdot p_{r,0} p_{s,1}$.
- **Case 3** ($p_{s,0} = p_{r,0}$ and $p_{s,1} > p_{r,1}$): Since $p_{r,0}$ and $p_{s,1}$ are relatively prime numbers, and $p_{s,0}$ and $p_{r,1}$ are relatively prime numbers, the beam alignment time is $M \cdot p_{r,0} p_{s,1} = M \cdot p_{r,1} p_{s,0}$.

As a result, each combination of beam pairs occurs once and does not repeat within $M \cdot \max(p_{r,0}, p_{s,1}) \max(p_{r,1}, p_{s,0})$ time slots. ■

In above lemma, the performance bound (worst case performance) to achieve beam assignment is characterized. In the following corollary, we further derive the mean latency to achieve beam alignment.

Corollary 1: Denote $H = M \cdot \max(p_{r,0}, p_{s,1}) \max(p_{r,1}, p_{s,0})$ as the worst case latency to achieve beam alignment through using an equal workload to perform beam sweeping, the mean latency to achieve beam alignment is given by

$$E[T] = N_r N_s + H \left(1 - \frac{1}{N_r N_s}\right)^M. \quad (11)$$

Proof: This proof can be done through direct derivation as follows.

$$\begin{aligned} E[T] &= \sum_{t=1}^H t \cdot \Pr\{T = t\} \\ &= \sum_{t=1}^M t \cdot \Pr\{T = t\} + \sum_{t=M+1}^H t \cdot \Pr\{T = t\} \\ &= \sum_{t=1}^M t \cdot \frac{1}{N_r N_s} \left(1 - \frac{1}{N_r N_s}\right)^{t-1} + \sum_{t=M+1}^H t \cdot \Pr\{T = t\} \\ &\leq \sum_{t=1}^M t \cdot \frac{1}{N_r N_s} \left(1 - \frac{1}{N_r N_s}\right)^{t-1} + H \sum_{t=M+1}^H \Pr\{T = t\} \\ &= N_r N_s + H \cdot \Pr\{T > M\} \\ &= N_r N_s + H \left(1 - \frac{1}{N_r N_s}\right)^M. \end{aligned} \quad (12)$$

V. OPTIMUM BEAM SWEEPING SEQUENCES WHEN ONLY A COMMON GEOGRAPHIC REFERENCE IS AVAILABLE FOR S1

As aforementioned, when a common geographic reference is available, there is a corresponding transmission beam direction and a reception beam direction to achieve beam alignment at any location. Denote T_{S1} as the minimum latency to achieve beam alignment,

$$T_{S1} = \inf\{t : B_r(t) = i^* \text{ and } B_s(t) = j^*\}. \quad (13)$$

Since the location of a receiver z is a random variable with the distribution $\Pr\{Y_r = z\} = y_z$, T_{S1} is also a random variable. Therefore, our goal turns out to design beam sweeping sequences that is able to approach the mean of T_{S1} (denoted by $E[T_{S1}]$). For this purpose, we should characterize $E[T_{S1}]$ in the following lemma.

Lemma 3: The mean of T_{S1} is given by

$$E[T_{S1}] = \sum_{t=1}^L t \sum_{z=0}^{\max\{N_r, N_s\}-1} \left(y_z \frac{1}{N_r N_s}\right) \left(1 - y_z \frac{1}{N_r N_s}\right)^{t-1}, \quad (14)$$

where $L = \max\{L_s, L_r\}$.

Proof: This lemma can be obtained through direct derivation. ■

To approach $E[T_{S1}]$, the following two propositions derive the principles of the position and workload of the optimum beam direction arrangement.

Proposition 1: All beam directions associated with the receiver location with a higher probability should be arranged at preceding positions in a beam sweeping sequence.

Proof: To minimize $E[T_{S1}]$ in (14), the probability of beam alignment for small t should be maximized. To this end, the beam direction associated with the present highest y_z should be arranged at preceding positions of a beam sweeping sequence, so as to increase the dominating factor $y_z \frac{1}{N_r N_s}$ and minimize $E[T_{S1}]$. ■

In addition to the position of beam directions in a beam sweeping sequence, we also desire to know how does the workload of each beam direction in a beam sweeping sequence affect $E[T_{S1}]$. Let $[z_0, z_1, \dots, z_{N_r-1}]$ denote ordered indices of the receiver locations, where z_0 is the location index with the largest y_z , z_1 is the location index with the second largest y_z , and so on. We also denote $[B_{z_0}, B_{z_1}, \dots, B_{z_{N_r-1}}]$ as beam direction indices associated with the location indices $[z_0, z_1, \dots, z_{N_r-1}]$. If the beam direction B_{z_0} is selected from $t = 1$ to $t = L \Pr\{B_{z_0}\}$, where $\Pr\{B_{z_i}\}$ is the probability to select the i th beam direction B_{z_i} , and B_{z_1} is selected from $t = L \Pr\{B_{z_0}\} + 1$ to $t = L[\Pr\{B_{z_0}\} + \Pr\{B_{z_1}\}]$, and so on, then

$$\begin{aligned} E[T_{S1}] &= \sum_{t=1}^{L \Pr\{B_{z_0}\}} t \left(y_{z_0} \Pr\{B_{z_0}\} \frac{1}{N_s} \right) \\ &\quad \cdot \left(1 - y_{z_0} \Pr\{B_{z_0}\} \frac{1}{N_s} \right)^{t-1} \\ &\quad + \sum_{t=L \Pr\{B_{z_0}\} + 1}^{L[\Pr\{B_{z_0}\} + \Pr\{B_{z_1}\}]} t \left(y_{z_1} \Pr\{B_{z_1}\} \frac{1}{N_s} \right) \\ &\quad \cdot \left(1 - y_{z_1} \Pr\{B_{z_1}\} \frac{1}{N_s} \right)^{t-L \Pr\{B_{z_0}\}} \\ &\quad \cdot \left(1 - y_{z_0} \Pr\{B_{z_0}\} \frac{1}{N_s} \right)^{t-L \Pr\{B_{z_0}\}} + \dots \end{aligned} \quad (15)$$

If the workload $\Pr\{B_{z_i}\}$ changes, the upper limit of the summation in (15) also changes. (15) thus reveals

that $E[T_{S1}]$ is affected by the workload of each beam direction.

Proposition 2: Using an equal workload to generate a beam sweeping sequence is better than using any other workload arrangement.

Proof: If the workload $\Pr\{B_{z_i}\}$ of a beam sweeping sequence is proportional to y_{z_i} , a larger workload may decrease the probability of beam alignment to be achieved at the next beam direction. In fact, arranging a larger workload at a particular beam direction only increases little probability of beam alignment at this beam direction, since the probability of beam alignment is smaller when t increases. However, arranging a larger workload at a particular beam direction may largely degrade the probability of beam alignment at the next beam direction. This argument thus suggests the optimality of the equal workload. ■

VI. OPTIMUM BEAM SWEEPING SEQUENCES WHEN BOTH A COMMON GEOGRAPHIC REFERENCE AND THE TRANSMITTER BEAM SWEEPING SEQUENCE ARE AVAILABLE FOR S4

For S4, a receiver knows not only which beam direction is selected at all time t , but also which beam direction achieves beam alignment. The receiver only needs to wait until the transmitter selects the beam direction to achieve beam alignment. We therefore can reuse **Algorithm 1** to generate the beam sweeping sequence at the transmitter side and make it a common knowledge. When the beam sweeping sequence at the transmitter side is a common knowledge, we can observe from (14) that the upper bound of the beam alignment latency is reached when all beam directions at the transmitter side have been present in the beam sweeping. An optimum beam sweeping sequence design therefore should sweep over all the beam directions as fast as possible. For this purpose, in the design of **Algorithm 1**, there are always $\lceil N_s/2 \rceil$ differences between two 0-sequences at the transmitter side.

Take Fig. 2 as an illustration example, in which N_s is 5. If one 0-sequence is (1, 2, 3, 4, 5, ...) and another 0-sequence is (2, 3, 4, 5, 1, ...), then the difference between each element of these two 0-sequences is one, which is less than $\lceil N_s/2 \rceil = 3$. In this case, the generated beam sweeping sequence is (1, 2, 2, 3, 3, 4, 4, 5, 5, 1, ...). As a result, it takes eight time slots for a transmitter to sweep over all beam directions. On the other hand, if one 0-sequence is (1, 2, 3, 4, 5, ...) and another 0-sequence is designed to (4, 5, 1, 2, 3, ...), then the difference between each element of these two 0-sequences is three, which satisfies $\lceil N_s/2 \rceil = 3$. In this case, the generated beam sweeping sequence is (1, 4, 2, 5, 3, 1, ...). As a result, it takes only five time slots for a transmitter to sweep over all beam directions.

The spirit of this design is to guarantee that all beam directions at the transmitter side can be swept during the minimum time duration. For this design to reuse **Algorithm 1**, the upper bound of the beam alignment latency is $T_{S4} \leq M \lceil N_s/2 \rceil / 2$.

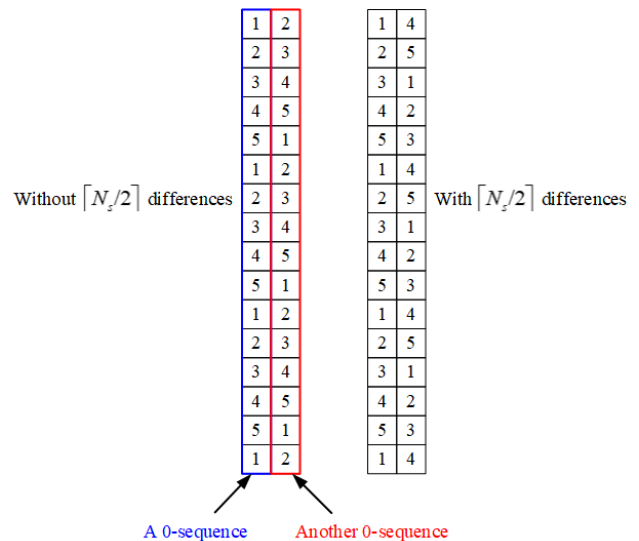


FIGURE 2. An example of two 0-sequences with and without $\lceil N_s/2 \rceil$ differences.

VII. PERFORMANCE EVALUATION

A. LATENCY PERFORMANCE OF S2 AND S3

We first evaluate the latency performance of the proposed beam sweeping scheme for S2 and S3, as these two situations align with the case of initial access. As aforementioned, if all beam directions are swept with an equal workload, then the ideal latency performance is $O(N_s N_r)$. However, if N_s and N_r are not relatively prime numbers, then the occurrence beam alignment cannot be guaranteed. By applying the proposed scheme with the facilitation with 4-bit cyclically unique codewords, then the worst case latency can be bounded by (10). To evaluate the performance of the proposed scheme comparing with these performance bounds, in Fig. 3 to Fig. 5, the performances in terms of average latency to achieve beam alignment over 10,000 repeated experiments under different N_s and N_r values are provided. The upper bound of latency performance derived in (10) and $N_s N_r$ are provided above each bar in Fig. 3 to Fig. 5.

We can observe from Fig. 3 to Fig. 5 that the beam alignment latency increases as N_r and N_s increase, which also show that the beam alignment latency of the proposed scheme effectively approaches the ideal performance. The derived worst case performance in (10) also provides an effective bound for the beam alignment latency.

B. LATENCY PERFORMANCE OF S1

We next evaluate the latency performance of the proposed beam sweeping scheme for S1. In this performance evaluation, it is assumed there are four ($Z = 4$) possible locations where a receiver can move to, and $N_r = 4$. If a receiver is at location $z = 0$, then a receiver selecting the beam direction $i = 0$ can achieve beam alignment. If a receiver is at location $z = 1$, then a receiver selecting the beam direction $i = 1$ can achieve beam alignment, and so on. The distribution of z is assumed to be $[y_{z_0}, y_{z_1}, y_{z_2}, y_{z_3}] = [0.5, 0.2, 0.2, 0.1]$.

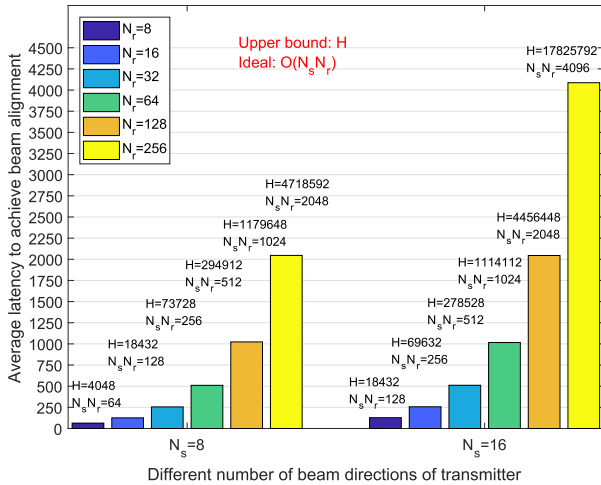


FIGURE 3. Average latency performance of beam alignment when $N_s = 8$ and 16.

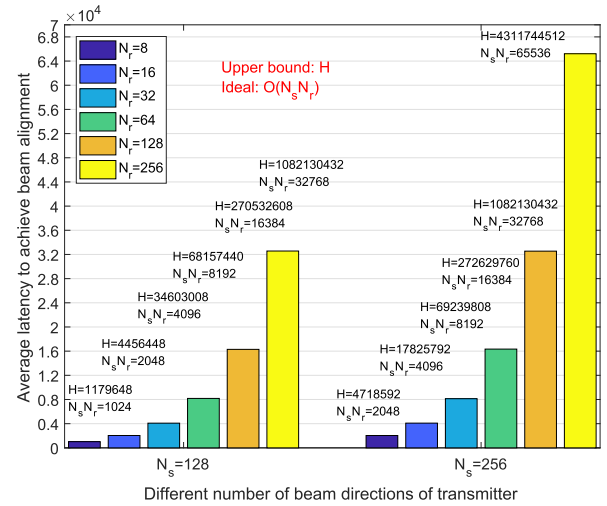


FIGURE 5. Average latency performance of beam alignment when $N_s = 128$ and 256.

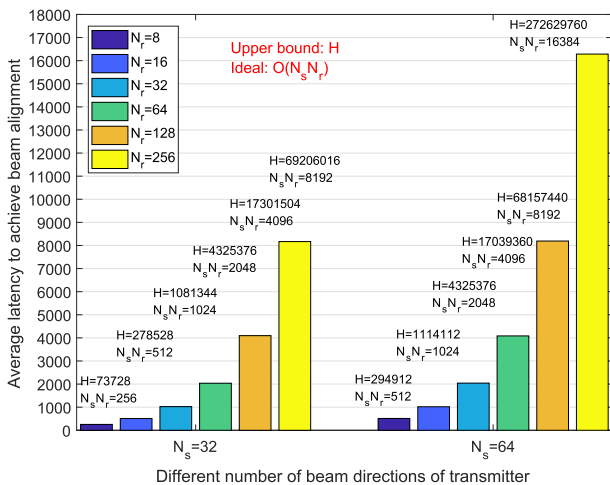


FIGURE 4. Average latency performance of beam alignment when $N_s = 32$ and 64.

To evaluate the performance of $E[T_{S1}]$, the following four scenarios are considered.

- **Scenario 1.** The workload of each beam direction in the beam sweeping sequence at the receiver side is proportional to the distribution of receiver’s location. That is, if the period of the beam sweeping sequence is L_r , then the workloads of the four beam directions are $[0.5L_r, 0.2L_r, 0.2L_r, 0.1L_r]$. In addition, all beam directions associated with the location with a higher probability are arranged at preceding positions in the beam sweeping sequence. Taking $L_r = 10$ as an illustration example, the beam sweeping sequence is designated to $(0, 0, 0, 0, 0, 1, 1, 2, 2, 3, \dots)$.
- **Scenario 2.** Regardless of the receiver’s location distribution, an equal workload is adopted to arrange each beam direction in the beam sweeping sequence. That is, the workloads of the four directions are $[0.25L_r, 0.25L_r, 0.25L_r, 0.25L_r]$. All beam directions associated

with the location with a higher probability are arranged at preceding positions in the beam sweeping sequence. That is, for $L_r = 10$, the beam sweeping sequence is $(0, 0, 0, 1, 1, 1, 2, 2, 3, 3, \dots)$. Please note that this scenario is the proposed scheme.

- **Scenario 3.** An equal workload is adopted to arrange each beam direction, and all beam direction associated with the location with a lower probability are arranged at preceding positions in the beam sweeping sequence. That is, for $L_r = 10$, the beam sweeping sequence is $(3, 3, 2, 2, 1, 1, 1, 0, 0, 0, \dots)$.
- **Scenario 4.** An equal workload is adopted to arrange each beam direction, and at least one beam direction associated with the location with a higher probability is arranged at preceding positions of at least one beam direction associated with the location with a lower probability. That is, for $L_r = 10$, the beam sweeping sequence is $(0, 1, 2, 3, 0, 1, 2, 3, 0, 1, \dots)$.

In Fig. 6 and Fig. 7, the performances in terms of $E[T_{S1}]$ for different considered scenarios are shown, we can observe that the performance of the proposed scheme (i.e., Scenario 2) outperforms other scenarios for different periods of the beam sweeping sequences. This result thus fully demonstrates the optimality of the proposed scheme.

Besides the considered distribution $[0.5, 0.2, 0.2, 0.1]$, we further adopt another distribution of z in which each location is reached with an equal probability (i.e., $[0.25, 0.25, 0.25, 0.25]$). For such distribution of z , the following scenarios are further considered in the performance evaluation.

- **Scenario 5.** The workloads of the four beam directions are the same as that in Scenario 1, even the distribution of z has been changed (i.e., $[0.5L_r, 0.2L_r, 0.2L_r, 0.1L_r]$). In addition, the beam direction arrangement is also the same as that in Scenario 1. Taking $L_r = 10$ as an illustration example, the beam sweeping sequence is designated to $(0, 0, 0, 0, 0, 1, 1, 2, 2, 3, \dots)$.

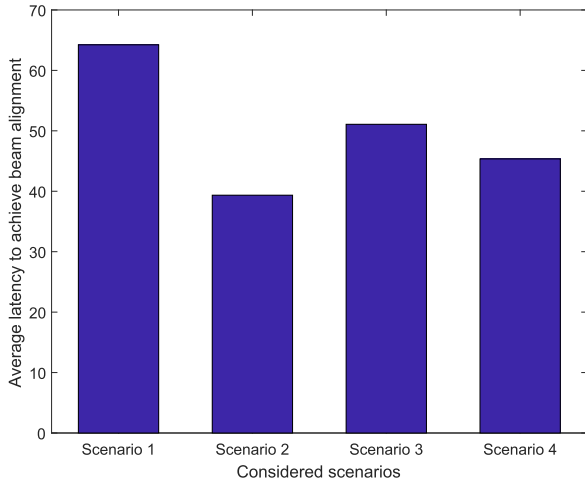


FIGURE 6. Average latency performance of beam alignment when $L_r = 10$ (Scenario 2 is the proposed scheme).

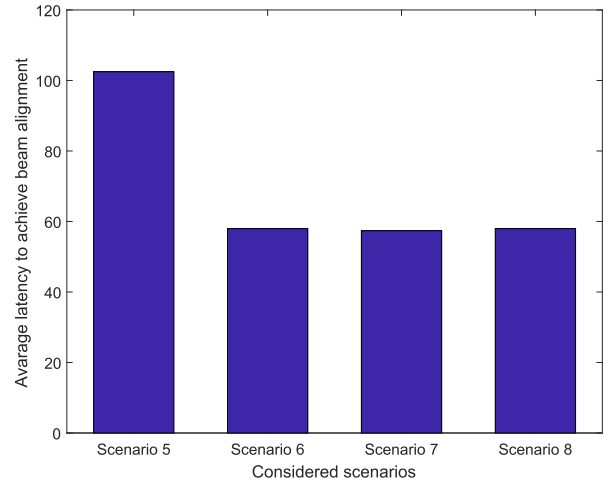


FIGURE 8. Average latency performance of beam alignment when $L_r = 10$ (Scenario 6 is the proposed scheme).

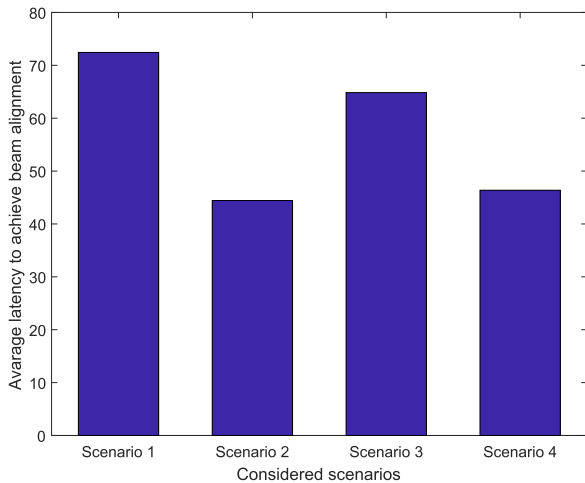


FIGURE 7. Average latency performance of beam alignment when $L_r = 20$ (Scenario 2 is the proposed scheme).

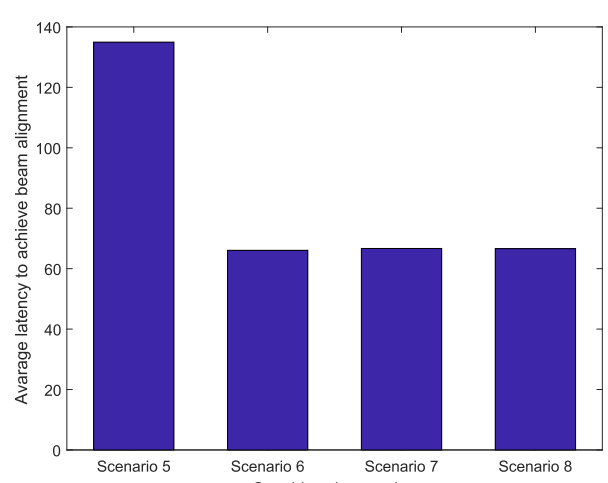


FIGURE 9. Average latency performance of beam alignment when $L_r = 20$ (Scenario 6 is the proposed scheme).

- **Scenario 6.** Regardless of the receiver’s location distribution, an equal workload is adopted to arrange each beam direction in the beam sweeping sequence. That is, the workloads of the four directions are $[0.25L_r, 0.25L_r, 0.25L_r, 0.25L_r]$. All beam directions associated with the location with a higher probability are arranged at preceding positions in the beam sweeping sequence. That is, for $L_r = 10$, the beam sweeping sequence is $(0, 0, 0, 1, 1, 1, 2, 2, 3, 3, \dots)$.
- **Scenario 7.** An equal workload is adopted to arrange each beam direction, and all beam direction associated with the location with a lower probability are arranged at preceding positions in the beam sweeping sequence. That is, for $L_r = 10$, the beam sweeping sequence is $(3, 3, 2, 2, 1, 1, 1, 0, 0, 0, \dots)$.
- **Scenario 8.** An equal workload is adopted to arrange each beam direction. For $L_r = 10$, the beam sweeping sequence is $(0, 1, 2, 3, 0, 1, 2, 3, 0, 1, \dots)$.

The performance of $E[T_{s_1}]$ under such uniform distribution of z is shown in Fig. 8 and Fig. 9 with $L_r = 10$ and $L_r = 20$, respectively. Since z is uniformly distributed, different position arrangements of beam directions may not impact the latency performance. Therefore, the performances in **Scenario 6**, **Scenario 7** and **Scenario 8** adopting an equal workload are around the same level. However, since an equal workload is not adopted in **Scenario 6**, the performance is significantly degraded.

C. LATENCY PERFORMANCE OF S4

Finally, we evaluate the latency performance of the proposed beam sweeping scheme for S4. In this performance evaluation, **Algorithm 2** is reused to generate the beam sweeping sequence at the transmitter side, and a cyclically unique codeword with $M = 4$ is adopted. In addition, two scenarios are considered.

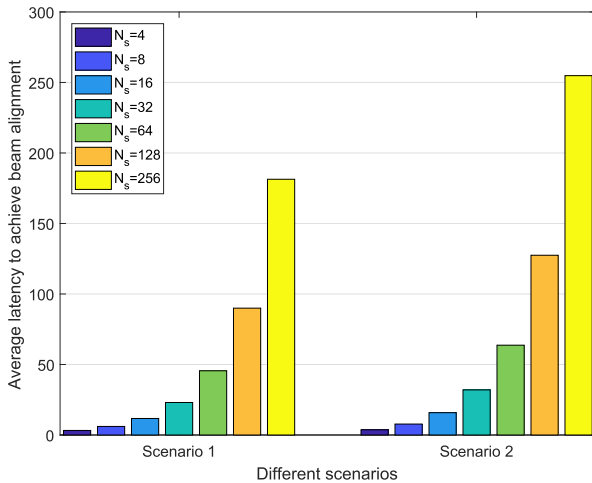


FIGURE 10. Average latency performance of beam alignment under different N_s and N_r (Scenario 1 is the proposed scheme).

- **Scenario 1.** In this scenario, there are $\lceil N_s/2 \rceil$ differences of beam directions between two 0-sequences. This scenario is our proposed scheme.
- **Scenario 2.** In this scenario, there are no $\lceil N_s/2 \rceil$ differences of beam directions between two 0-sequences.

In Fig. 10, the average latency of beam alignment in these two scenarios are shown under different N_s , and N_r is set to $N_r = N_s$. We can observe from Fig. 10 that proposed scheme outperforms the scheme without introducing $\lceil N_s/2 \rceil$ differences of beam directions between two 0-sequences. This result thus fully demonstrates the effectiveness of the proposed scheme.

VIII. CONCLUSION

In this paper, we derive the latency-optimal beam sweeping sequences for a transmitter and a receiver under four situations: S1) Only a common geographic reference is available; S2) Only the beam sweeping sequence at the transmitter side is available; S3) None of a common geographic reference and the beam sweeping sequence at the transmitter side is available; S4) Both a common geographic reference and the beam sweeping sequence at the transmitter side are available. For S2 and S3 in which a common geographic reference is not available, **Algorithm 1** and **Algorithm 2** are developed based on time shift sequences with cyclically unique codewords to generate the latency-optimal beam sweeping sequences at the transmitter side and receiver side, respectively. For S1 in which a common geographic reference is available, two principles for the latency-optimal beam sweeping sequence designs are derived: 1) All beam directions associated with the receiver location with a higher probability should be arranged at preceding positions in a beam sweeping sequence, and 2) using an equal workload to generate a beam sweeping sequence is better than using any other workload arrangement. For S4, **Algorithm 1** and **Algorithm 2** are proposed to be reused in generating the beam sweeping sequences at

the transmitter side and receiver side, respectively. In the meantime, we propose that there should always be $\lceil N_s/2 \rceil$ differences of beam directions between two 0-sequences. Our simulation results fully show that the proposed schemes can effectively approach the ideal performance, to demonstrate the practicability for the next generation driving use cases using mmWave carriers.

REFERENCES

- [1] C.-Y. Chang, H.-C. Yen, and D.-J. Deng, "V2V QoS guaranteed channel access in IEEE 802.11p VANETs," *IEEE Trans. Dependable Secure Comput.*, vol. 13, no. 1, pp. 5–17, Jan./Feb. 2016.
- [2] A. Vinel, "3GPP LTE versus IEEE 802.11p/WAVE: Which technology is able to support cooperative vehicular safety applications?" *IEEE Wireless Commun. Lett.*, vol. 1, no. 2, pp. 125–128, Apr. 2012.
- [3] C. Campolo, A. Molinaro, A. Vinel, and Y. Zhang, "Modeling event-driven safety messages delivery in IEEE 802.11p/WAVE vehicular networks," *IEEE Commun. Lett.*, vol. 17, no. 12, pp. 2392–2395, Dec. 2013.
- [4] Q. Wang, S. Leng, H. Fu, and Y. Zhang, "An IEEE 802.11p-based multichannel MAC scheme with channel coordination for vehicular ad hoc networks," *IEEE Trans. Intell. Transp. Syst.*, vol. 13, no. 2, pp. 449–458, Jun. 2012.
- [5] S.-Y. Lien, D.-J. Deng, H.-L. Tsai, Y.-P. Lin, and K.-C. Chen, "Vehicular radio access to unlicensed spectrum," *IEEE Wireless Commun.*, vol. 24, no. 6, pp. 46–54, Dec. 2017.
- [6] D.-J. Deng, S.-Y. Lien, C.-C. Lin, S.-C. Hung, and W.-B. Chen, "Latency control in software-defined mobile-edge vehicular networking," *IEEE Commun. Mag.*, vol. 55, no. 8, pp. 87–93, Aug. 2017.
- [7] H. Seo, K.-D. Lee, S. Yasukawa, Y. Peng, and P. Sartori, "LTE evolution for vehicle-to-everything services," *IEEE Commun. Mag.*, vol. 54, no. 6, pp. 22–28, Jun. 2016.
- [8] *Study on Enhancement of 3GPP Support for 5G V2X Services*, document TR 22.886 V16.1.1, 3GPP, Sep. 2018.
- [9] *Service Requirements for Enhanced V2X Scenarios*, document TS 22.186 V16.0.0, 3GPP, Sep. 2018.
- [10] S.-Y. Lien, S.-L. Shieh, Y. Huang, B. Su, Y.-L. Hsu, and H.-Y. Wei, "5G new radio: Waveform, frame structure, multiple access, and initial access," *IEEE Commun. Mag.*, vol. 55, no. 6, pp. 64–71, Jun. 2017.
- [11] S.-Y. Lien, S.-C. Hung, D.-J. Deng, C.-L. Lai, and H.-L. Tsai, "Low latency radio access in 3GPP local area data networks for V2X: Stochastic optimization and learning," *IEEE Internet Things J.*, to be published.
- [12] S.-Y. Lien, S.-C. Hung, and K.-C. Chen, "Optimal radio access for fully packet-switching 5G networks," in *Proc. IEEE Int. Conf. Commun. (ICC)*, Jun. 2015, pp. 3921–3926.
- [13] S.-Y. Lien, S.-C. Hung, D.-J. Deng, and Y. J. Wang, "Efficient ultra-reliable and low latency communications and massive machine-type communications in 5G new radio," in *Proc. IEEE Global Commun. Conf.*, Dec. 2017, pp. 1–7.
- [14] T. S. Rappaport et al., "Millimeter wave mobile communications for 5G cellular: It will work!" *IEEE Access*, vol. 1, pp. 335–349, 2013.
- [15] S. Rangan, T. S. Rappaport, and E. Erkip, "Millimeter-wave cellular wireless networks: Potentials and challenges," *Proc. IEEE*, vol. 102, no. 3, pp. 366–385, Mar. 2014.
- [16] Z. Pi and F. Khan, "An introduction to millimeter-wave mobile broadband systems," *IEEE Commun. Mag.*, vol. 49, no. 6, pp. 101–107, Jun. 2011.
- [17] A. Ghosh et al., "Millimeter-wave enhanced local area systems: A high-data-rate approach for future wireless networks," *IEEE J. Sel. Areas Commun.*, vol. 32, no. 6, pp. 1152–1163, Jun. 2014.
- [18] J.-C. Chen, "Energy-efficient hybrid precoding design for millimeter-wave massive MIMO systems via coordinate update algorithms," *IEEE Access*, vol. 6, pp. 17361–17367, 2018.
- [19] J. Rodríguez-Fernández, N. González-Prelcic, K. Venugopal, and R. W. Heath, Jr., "Frequency-domain compressive channel estimation for frequency-selective hybrid millimeter wave MIMO systems," *IEEE Trans. Wireless Commun.*, vol. 17, no. 5, pp. 2946–2960, May 2018.
- [20] J. Jin, Y. R. Zheng, W. Chen, and C. Xiao, "Hybrid precoding for millimeter wave MIMO systems: A matrix factorization approach," *IEEE Trans. Wireless Commun.*, vol. 17, no. 5, pp. 3327–3339, May 2018.

- [21] J. Mo, P. Schniter, and R. W. Heath, Jr., "Channel estimation in broadband millimeter wave MIMO systems with few-bit ADCs," *IEEE Trans. Signal Process.*, vol. 66, no. 5, pp. 1141–1154, Mar. 2018.
- [22] C.-R. Tsai, Y.-H. Liu, and A.-Y. Wu, "Efficient compressive channel estimation for millimeter-wave large-scale antenna systems," *IEEE Trans. Signal Process.*, vol. 66, no. 9, pp. 2414–2428, May 2018.
- [23] F. Guidi, N. Decarli, D. Dardari, F. Mani, and R. D'Errico, "Millimeter-wave beamsteering for passive RFID tag localization," *IEEE J. Radio Freq. Identificat.*, vol. 2, no. 1, pp. 9–14, Mar. 2018.
- [24] F. Guidi, N. Decarli, D. Dardari, F. Mani, and R. D'Errico, "Passive millimeter-wave RFID using backscattered signals," in *Proc. IEEE Globecom Workshops (GC Wkshps)*, Dec. 2016, pp. 1–6.
- [25] P. Pursula, F. Donzelli, and H. Seppä, "Passive RFID at millimeter waves," *IEEE Trans. Microw. Theory Techn.*, vol. 59, no. 8, pp. 2151–2157, Aug. 2011.
- [26] B. Yin, Y. Chen, Z. Zhang, M. Wang, and S. Sun, "Beam discovery signal-based beam selection in millimeter wave heterogeneous networks," *IEEE Access*, vol. 6, pp. 16314–16323, 2018.
- [27] A. W. Mbugua, W. Fan, Y. Ji, and G. F. Pedersen, "Millimeter wave multi-user performance evaluation based on measured channels with virtual antenna array channel sounder," *IEEE Access*, vol. 6, pp. 12318–12326, 2018.
- [28] R. Pal, K. V. Srinivas, and A. K. Chaitany, "A beam selection algorithm for millimeter-wave multi-user MIMO systems," *IEEE Commun. Lett.*, vol. 22, no. 4, pp. 852–855, Apr. 2018.
- [29] A. Shahmansoori, G. E. Garcia, G. Destino, G. Seco-Granados, and H. Wymeersch, "Position and orientation estimation through millimeter-wave MIMO in 5G systems," *IEEE Trans. Wireless Commun.*, vol. 17, no. 3, pp. 1822–1835, Mar. 2018.
- [30] T. Nitsche, A. B. Flores, E. W. Knightly, and J. Widmer, "Steering with eyes closed: mm-Wave beam steering without in-band measurement," in *Proc. IEEE Conf. Comput. Commun. (INFOCOM)*, Apr./May 2015, pp. 2416–2424.
- [31] V. Va, J. Choi, T. Shimizu, G. Bansal, and R. W. Heath, Jr., "Inverse multipath fingerprinting for millimeter wave V2I beam alignment," *IEEE Trans. Veh. Technol.*, vol. 67, no. 5, pp. 4042–4058, May 2018.
- [32] S.-Y. Lien, C.-C. Chien, G. S.-T. Liu, H.-L. Tsai, R. Li, and Y. J. Wang, "Enhanced LTE device-to-device proximity services," *IEEE Commun. Mag.*, vol. 54, no. 12, pp. 174–182, Dec. 2016.
- [33] S.-Y. Lien, C.-C. Chien, F.-M. Tseng, and T.-C. Ho, "3GPP device-to-device communications for beyond 4G cellular networks," *IEEE Commun. Mag.*, vol. 54, no. 3, pp. 29–35, Mar. 2016.
- [34] N. C. Theis, R. W. Thomas, and L. A. DaSilva, "Rendezvous for cognitive radios," *IEEE Trans. Mobile Comput.*, vol. 10, no. 2, pp. 216–227, Feb. 2011.
- [35] L. Chen, K. Bian, L. Chen, C. Liu, J. M. J. Park, and X. Li, "A group-theoretic framework for rendezvous in heterogeneous cognitive radio networks," in *Proc. 15th ACM Int. Symp. Mobile Ad Hoc Netw. Comput.*, Aug. 2014, pp. 165–174.



SHAO-YU LIEN received the B.S. degree from National Taiwan Ocean University, in 2004, the M.S. degree from National Cheng Kung University, in 2006, and the Ph.D. degree from National Taiwan University, in 2011. He has been with the Department of Computer Science and Information Engineering, National Chung Cheng University, Taiwan, since 2017. His current research interests include 5G/6G mobile networks, cyber-physical systems, and configurable networks. He was a recipient of the IEEE ICC 2010 Best Paper Award, the URSI AP-RASC 2013 Young Scientist Award, the IEEE Communications Society Asia-Pacific Outstanding Paper Award, in 2014, and the Scopus Young Researcher Award (issued by Elsevier), in 2014.



YEN-CHIH KUO received the B.S. degree from National Formosa University, in 2018. His current research interests include 5G/6G mobile networks and mmWave network designs.



DER-JIUNN DENG (M'10) received the Ph.D. degree in electrical engineering from National Taiwan University, in 2005. He joined the Department of Computer Science and Information Engineering, National Changhua University of Education, as an Assistant Professor, in 2005, and then became a Distinguished Professor, in 2016. In 2018, he was seconded to Overseas Chinese University as the Vice President for research and development for a period of one year. His research interests include multimedia communication, quality-of-service, and wireless local network. He has received a number of research awards, such as the Research Excellency Award of the National Changhua University of Education, the Outstanding Faculty Research Award of the National Changhua University of Education, the ICS 2014 Best Paper Award, the NCS 2017 Best Paper Award, and the Chinacom 2017 Best Paper Award. He is the Co-Editor-in-Chief of the EAI Endorsed *Transactions on IoT* and the *Journal of Computers*. He serves as an Associate Editor for the *IEEE Network Magazine* and the *International Journal of Communication Systems*. He also served or is serving on several program chairs, symposium chairs, and technical program committees for IEEE and other international conferences.



HUA-LUNG TSAI received the B.S. degree in electrical engineering from the National Taiwan University of Science and Technology, in 2000, the M.S. degree in electrical engineering from National Chung Cheng University, in 2005, and the Ph.D. degree in communication engineering from National Taiwan University, in 2015. He joined the Information and Communications Research Laboratories, Industrial Technology Research Institute, in 2012. Since 2014, he has been actively involving in the development and standardization of 3GPP LTE-Advanced and 5G technologies. His research interests include physical and MAC layer protocols for device-to-device, V2X communications, and new radio access technology.



ALEXEY VINEL was born in Saint-Petersburg, Russia, in 1983. He received the Ph.D. degree in telecommunication systems and computer networks from the Institute for Information Transmission Problems, Russian Academy of Sciences, in 2007. In 2010, he joined the Tampere University of Technology, Finland, as a Researcher. In 2013, he started with Halmstad University as a Guest Professor, where he was appointed as a Professor, in 2015. He was the Group Leader and a Senior Researcher with the Saint-Petersburg Institute for Informatics and Automation, Russian Academy of Science. He has been an IEEE Senior Member, since 2012. He received the Alexander von Humboldt Fellowship, Germany, in 2008. He has been the chairman of several international conferences and workshops, for example ITST and Nets4Cars. He has also been on the Editorial Board of top ranked scientific journals, such as the IEEE TRANSACTIONS ON DEPENDABLE AND SECURE COMPUTING and the IEEE COMMUNICATIONS LETTERS.



ABDERRAHIM BENSLIMANE received the B.S. degree from the University of Nancy, in 1987, the M.S. degree from the Franche-Comte University of Besançon, in 1989, and the Ph.D. degree from DEA in 1993, all in computer science. He was the Head of the Computer Laboratory, Computer Networks and Multimedia Applications Group (RAM), Avignon, from 2001 to 2009. He has been a Professor of computer science with the University of Avignon, France, since 2001. He served as a Coordinator of the Faculty of Engineering, French University, Egypt. He has been an Associate Professor with the University of Technology of Belfort-Montbéliard, since 1994. He has been involved in many national and international projects, ANR, French-International bilateral projects, PHC and H2020. He is currently working on the conception and performance evaluation of protocols for security, privacy, and trustiness in the Internet of Things and vehicles. His research interests include the development of communication protocols with the use of graph theory for mobile and wireless networks. He has authored more than 160 refereed international publications (books, proceedings, journals, and conferences) in all those domains. He is a Student Member of the IEEE. He was a member of the French Council of Universities (CNU Section 27), from 2003 to 2007. He was a Board

Committee Member, a Vice Chair of student activities of the IEEE France Section/Region 8, a Publication Vice Chair, and a Conference Vice Chair. He was attributed with the French Award of Scientific Excellency, from 2011 to 2014. He received the French Award of Doctoral Supervisions (2017–2021). He obtained the title to supervise researches (HDR 2000) from the University of Cergy-Pontoise, France. He participates in the steering and program committees of many IEEE international conferences. He is the Founder and has been serving as a General Chair for the IEEE WiMob, since 2005, and for iCOST and MoWNet international conferences, since 2011. He served as a Symposium Co-Chair/Leader in many IEEE international conferences, such as ICC, GLOBECOM, AINA, and VTC. He is currently the Chair of the ComSoc TC of Communication and Information Security. He is also the Chair of Communications and Information Security TC of the IEEE Communication Society. He has been recently a Technical International Expert with the French Ministry of Foreign and European Affairs, from 2012 to 2016. He is also the Head of the master Systèmes Informatiques Communicants: réseaux, services et sécurité. He is the Editor-in-Chief of *Multimedia Intelligence and Security* journal, an Area Editor of *Security and Privacy* (Wiley) journal, and an Editorial Member of the *IEEE Wireless Communication Magazine* and *Ad Hoc Networks* (Elsevier). He served as a guest editor of many special issues.

...